Rostral Cingulate Zone and correct response monitoring : ICA and source localization evidences for the unicity of correct– and error–negativities [1]

4.1 Introduction

Keeping our behavior adapted to an ever changing environment requires a constant evaluation of one's own performance. In this respect, errors play an essential role in this evaluation, since they strongly signal the need for adaptation. In the early 90's, Falkenstein *et al.* (1991) reported the existence of an EEG component peaking just after error commission in reaction time (RT) tasks (see also Gehring *et al.*, 1993) : This fronto-central negative wave starts just before the response, and peaks between 50 and 100 ms later. With conventional monopolar recordings, this activity has originally been observed only on errors and was hence interpreted as reflecting an "Error Detection" mechanism. Accordingly, it was named "Error Negativity" (Ne, Falkenstein *et al.*, 1991) or "Error-

1. article en cours de révision dans le journal *NeuroImage*.

Related Negativity" (ERN, Gehring *et al.*, 1993). Source localization approaches (Dehaene *et al.*, 1994; Herrmann *et al.*, 2004; Van Veen et Carter, 2002) and fMRI data (Debener *et al.*, 2005; Ullsperger et von Cramon, 2001) have pointed to a Rostral Cingulate Zone (RCZ, Ridderinkhof *et al.*, 2004a) generator of this activity. This generator would be more likely located within the anterior cingulate cortex (ACC) and/or the supplementary motor area (SMA) (Dehaene *et al.*, 1994; Ullsperger et von Cramon, 2001). This Ne was later included in more general models of response monitoring, and was re-interpreted as reflecting conflict monitoring (Yeung *et al.*, 2004, see however Burle *et al.*, 2008a).

The specificity of the Ne to errors was disputed by Vidal *et al.* (2000). These authors computed the Current Source Density (by applying the Laplacian operator), which has been shown to dramatically improve the spatial resolution of monopolar recordings (Babiloni *et al.*, 2001). Thanks to this methodological improvement, Vidal *et al.* (2000) evidenced that a similar activity was also observed on correct trials, albeit with smaller amplitude. They first analyzed some particular correct trials in which *partial errors* occurred : On such trials, although the correct response was given, electromyographic (EMG) recordings allow to reveal a small EMG burst on the muscles involved in the incorrect response (Burle *et al.*, 2002b; Coles *et al.*, 1985; Eriksen *et al.*, 1985). Vidal and colleagues observed a negative wave just after the onset of such partial errors with comparable latency and topography as the wave reported on errors (see Scheffers *et al.*, 1996 for similar data in a go/nogo task). More importantly, they also reported a similar negativity, of smaller amplitude though, just after the EMG leading to the correct response on pure correct trials (*i.e.* trials without any sign of incorrect EMG activation).

The negative activities obtained on errors, partial errors and pure correct trials had similar topographies, similar time-courses (after Laplacian transform), and their amplitude was shown to monotonically decrease from errors to pure correct, with partial errors in between. Based on these similarities, Vidal *et al.* (2000) argued that the N_C was of same nature as the Ne on errors.

Coles *et al.* (2001) disputed this view and argued that the negativity reported by Vidal *et al.* (2000) on correct trials was due to an artifact caused by the temporal overlap between stimulus-locked and response-locked activities. To address this point, Vidal *et al.* (2003a) visualized the single-trial dynamics of the stimulus and response evoked potentials as a function of the reaction time, and showed that the N_C was clearly response-locked and independent from stimulus-locked activities. Several other studies have reported a negative wave in correct trials (Falkenstein *et al.*, 2000; Luu *et al.*, 2000b; Mathalon *et al.*, 2002), and there is now a consensus on its existence.

The question remains, however, to determine whether the negativities recorded on correct and

error trials reflect the same functional and physiological mechanisms modulated in amplitude or whether they are completely different processes.

While the proposition that the negativities observed on pure correct, partial errors and errors reflect the same, modulated, mechanism (Vidal *et al.*, 2000, 2003a), is supported by the fact that the negativity on correct trials is also sensitive to the subject's performance (Luu *et al.*, 2000b; Ridderinkhof *et al.*, 2003; Allain *et al.*, 2004c; Hajcak *et al.*, 2005b), this view was disputed by Yordanova *et al.* (2004). These authors reported that on correct trials the negativity tended to be lateralized toward the hemisphere controlateral to the responding hand whereas the topography was more central for errors. Based on the difference in topography and in the time-frequency pattern of negativities on correct and erroneous trials, they concluded that the two negativities reflect different processes. The lateralization reported by Yordanova *et al.* (2004) might well be due, however, to an independent source. Indeed, following the motor lateralization induced by response execution processes (Vidal *et al.*, 2003b, see Burle *et al.*, 2004b for a review), the lateralization of the N_C observed by Yordanova *et al.* (2004) could be due to the propagation of the primary motor activity towards premotor areas (see Tandonnet *et al.*, 2005, Fig. 1) : If this pre-motor activity is of same amplitude for correct and errors trials, it may contribute more to the topography when the amplitude of the medial activity is lower, that is for correct trials. This may give the false impression of a lateralization limited to correct trials, although the same lateralized activity could also be present on errors, but less visible. In agreement with this view, a critical look at the figures 1 and 6 of Yordanova *et al.* (2004) shows that, even on errors, the iso-contour lines present a lateralization.

Clarifying this debate is theoretically important since none of the current models of cognitive control can easily account for the presence of a "N_C " on correct trials. Thus, if the negativity on correct trials were of the same nature as the negativity on errors, this would indicate that control processes operate gradually from correctness to errors. This would also open new perspectives and add new constraints on cognitive control modeling.

We therefore assessed the unicity of those negativities with Independent Component Analysis (ICA, Onton *et al.*, 2006) and source localization techniques (sLORETA, Pascual-Marqui, 2002).

Applied to EEG, ICA posits that the scalp activity is a linear combination of a limited set of elementary brain signals (the *independent components*). Based on the assumptions of temporal independence, ICA allows one to recover the mixture of components and hence to estimate the time course and the topography of each component. Of special interest in the present context, ICA *blindly* recovers the components, that is, it does so without any a priori assumptions about

the components (except that they must be maximally independent from each other). We reasoned that if the three negativities recorded on errors, partial errors and correct trials reflect the same modulated elementary brain activity, they should be captured by ICA in the same component. On the contrary, if they reflect different mechanisms, it would not be possible to find a single component accounting for these three waves.

In addition to the ICA argument, we also applied Source localization techniques to recover the generator(s) of the three activities. Indeed, although there is now strong arguments for an RCZ origin of the Ne on errors (Dehaene *et al.*, 1994; Debener *et al.*, 2005), no explicit localization of the negativities recorded on both partial errors and correct trials has been reported so far [2]. Obtaining similar localizations for these three activities would provide a strong argument in favor of the unicity of the phenomenon.

4.2 Materials and Methods

The data relative to the partial errors have been reported in a previous study for different purposes (see Burle *et al.*, 2008a where a detailed description of the experiment is available). The method will thus be briefly summarized, with emphasis on the aspects relevant for our current goals.

4.2.1 Subjects

Ten subjects aged from 20 to 31 years (mean : 25 years) volunteered for the experiment. All of them were right-handed and had normal or corrected-to-normal vision. According to the declaration of Helsinki, written informed consent before the start of the experiment was obtained from each subject.

4.2.2 Task, Recordings and EEG Data preprocessing

The subjects performed an Eriksen's flanker task (Eriksen et Eriksen, 1974). On each trial, three letters were presented to subjects who had to respond to the central one (target) while ignoring the others (distractors). They ran 20 experimental blocks of 128 trials each.

2. An indirect attempt was done by Vocat *et al.* (2008), however : although those authors did not explicitly attempt to localize the Ne-like on correct trials, they evaluated whether the solution found for errors could account for the activity on correct trials

Electroencephalographic activity (EEG) was recorded with 64 Ag/AgCl scalp electrodes (10-20 system positions, BIOSEMI Active-two electrodes, Amsterdam) and electromyographic activity (EMG) from the *flexor pollicis brevis* of each hand was recorded by paired surface Ag/AgCl electrodes. The sampling rate was 1024 Hz (filters : DC to 268 Hz, 3 dB/octave).

The vertical and horizontal EOG was recorded in order to correct eye movement artifacts by the statistical method of Gratton *et al.* (1983). All other artifacts were rejected after visual inspection of individual traces. The onset of the EMG activity was marked manually after visual inspection (for further details, see Burle *et al.*, 2008a).

The retained data were then downsampled to 256 Hz (with BrainAnalyzer, Munich), since the original sampling rate was too high to perform ICA.

4.2.3 EEG Data analysis

The trials were sorted into three categories based on responses and on EMG patterns : pure-correct, error and partial error trials (see Burle *et al.*, 2002b, 2008a for more details). Partial errors trials are characterized by the presence of a small EMG burst on the incorrect response side preceding the EMG burst leading to the correct response. The EEG data were epoched, time-locked to the EMG activity that led to the overt response, namely the correct EMG burst for pure correct trials and partial errors, and the supraliminal incorrect EMG for errors.

Since previous reports have shown that the negativity on correct trials is much easier to observe after Laplacian computation, we also applied this transformation to the monopolar data, for the sake of comparison. The signal was interpolated with spherical spline interpolation, and hence the second derivatives in two dimensions of space were computed. We choose 3 for the degree of the spline since this value minimizes errors, and the interpolation was computed with a maximum of 15 degrees for the Legendre polynomial (Perrin *et al.*, 1989). We assumed a radius of 10 cm for the sphere representing the head, rather than the unrealistic default radius of 1 m assumed by BrainAnalyzer. With such a realistic radius, the most suitable unit is $\mu V/cm^2$.

4.2.4 Blind Source Separation (BSS) : General Principle

ICA algorithm performs a "Blind Source Separation" (BSS) of the signal. Applied to EEG, BSS posits that the activities $x_i(t)$ recorded on each sensors i (among I) at time t can be decomposed as a sum of elementary components defined as the product of a topography ($\alpha_{ij} \in \mathbb{R}^I$, representing the contribution of the component to each of the i electrodes) and a time course $s_j(t) \in \mathbb{R}^T$ (where

I corresponds to the number of sensors, J the number of components with $J \leqslant I$, and T the number of time samples) :

$$x_i(t) = \sum_{j=1}^{J} \alpha_{ij} s_j(t) \tag{4.1}$$

Generally speaking, the goal of BSS is to recover both the α_{ij} and the $s_j(t)$ knowing only the realization across time of the signal $x_i(t)$. This problem can also be formalized in matrix terms and becomes :

$$\mathbf{X} = \mathbf{A} \cdot \mathbf{S} \tag{4.2}$$

where $\mathbf{X} \in \mathbb{R}^{I \times T}$ is the observation matrix, $\mathbf{A} \in \mathbb{R}^{I \times J}$ is the mixing matrix and $\mathbf{S} \in \mathbb{R}^{J \times T}$ is the matrix of the components time course (*i.e.* the "sources" in the BSS terminology [3]).

Thus, BSS decomposes the input matrix $\mathbf{X}$ into the product of the two matrices $\mathbf{A}$ and $\mathbf{S}$. The decomposition of the $\mathbf{X}$ matrix is not unique, however, and additional constraints are needed.

One widely used constraint is that the sources must be statistically maximally independent. Such an approach is usually called "Independent Component Analysis". One way to quantify the independence between time series is to compute their mutual information (Bell et Sejnowski, 1995) and the `infomax` algorithm (used in the current study, see below) search for the $\mathbf{S}$ matrix whose mutual information across components is minimal.

Applied to EEG, ICA aims at recovering *elementary* brain activities that are mixed at the sensors level because of volume conduction and diffusion effects, without any modeling of such conduction and diffusion effects (Jung *et al.*, 2001).

4.2.5 ICA in the present study

Since, by demixing the observation matrix, ICA aims at recovering the *elementary* brain activities, we used ICA to address the unicity of the Ne and Ne-like observed on errors, partial errors and correct trials. Translated to ICA, the question of unicity becomes whether ICA decomposition can find a *single* component (although potentially with different temporal dynamic) accounting for the waves observed on the three categories of trials. In other words, can ICA *blindly* attribute

3. For the sake of clarity, we will consistently use the term "component" for the product of topography and time of course. We will use the word "generator" for the cortical activities reconstructed by source localization. Although, by applying ICA, one hopes that the recovered "components" will correspond to brain "generators", it is important to keep the two concepts separated.

a single brain origin to the three waves ? Addressing this question was performed in four steps, as detailed below.

First step : construction of the matrices. We first selected all the trials that were identified as correct, partial error or error trials. Partial errors were identified based on the EMG data. We removed trials contaminated by artifacts (see Burle *et al.*, 2008a for more details on artifact rejection). The selected trials were then segmented into epochs from -400 to +400 ms, centered on the EMG onset that triggered the overt response, either correct (correct and partial error trials) or incorrect (errors). Trials were then concatenated to form the $\mathbf{X}$ matrix of size $64 \times T$ (where 64 is the number of electrodes, and T is equal to `Number_of_trials` $\times$ `Time_sample_per_trials`). One single $\mathbf{X}$ matrix containing all the trials was built for each of the 10 subjects with the monopolar data. The individual matrices were of slightly different sizes since T depends on the number of trials included. Note that these data matrices are mainly composed of correct trials (76.8% on average) compared to errors and partial errors trials (5.2% and 18% on average, respectively).

Second step : ICA on individual matrices. ICA was applied to each of the $\mathbf{X}$ matrices. ICA computations were performed with the `runica()` function as implemented in the EEGLAB software (Delorme et Makeig, 2004) which is derived from the Infomax ICA algorithm (Bell et Sejnowski, 1995). This returned 64 components per subject.

Third step : searching for the component accounting for errors. We searched for the component that could account for the Ne on errors (see Debener *et al.*, 2005). As already indicated, an component is defined as a topography and a time course. An component was thus selected if its averaged time-course *on errors* presented a clear phasic activity whose projection on the scalp was of negative polarity at fronto-central sites (see Fig. 4.2 below for an example). The selected component accounting for the Ne will be termed Ne_IC_S for each subject S. Note that components were selected without any reference to correct trials.

Fourth step : Averaging of the selected component for partial error and correct trials. Once the Ne_IC_S, accounting for the Ne on errors, had been identified, we averaged the time course of Ne_IC_S for partial errors and correct trials. Based on these averages, we sought whether the Ne_IC_S could also account for the negativities observed on partial errors and on correct trials. To do so, we compared the component averages to both monopolar and Laplacian averages on the same trials.

4.2.6 Source Localization

To further probe similarities and differences between the negativities observed in the three categories of trials, we searched for the brain regions responsible for the genesis of those activities. Although source localization on errors has already been performed on several studies, to the best of our knowledge, the generator of the negativities on partial errors and on correct trials have never been localized so far. We thus sought for the generator of these three waves thanks to the standardized Low Resolution Electromagnetic Tomography (sLORETA) method, which implements a normalized form of the minimum norm constraint (see Pascual-Marqui, 2002 for technical details).

4.3 Results

4.3.1 Behavioral Data

Percentages of errors, partial errors and correct trials were respectively 5.2%, 18% and 76.8%, in average. The RTs associated with these three types of trials were significantly different ($F(2,18) = 84.6, P < 0.001$), with the shortest RTs obtained for errors (342 msec), followed by pure-correct trials (382 msec) and partial errors (445 msec). The typical compatibility effects have been replicated, and are presented in more details in Burle *et al.* (2008a).

4.3.2 EEG Data

This section will be organized as follows : we will first present the monopolar data for comparison with the literature. We will then present the Laplacian data, since this transformation permits to reveal the negativity on correct trials. We will then present the ICA data, and finally the source localization results.

Monopolar data

Fig. 4.1A presents the monopolar grand averages obtained over FCz for errors (blue line), partial errors (green) and correct trials (red), time-locked to the relevant EMG activity onset (see above). The presented data replicates results already published, showing a clear negative wave for errors (Falkenstein *et al.*, 1991; Gehring *et al.*, 1993) and partial errors (Scheffers *et al.*, 1996; Vidal *et al.*, 2000) shortly after EMG onset. The amplitude of this wave was higher for errors (14.4 μV) than for partial errors (7.05 μV, $F(1,9) = 13.26; p < 0.01$). As usually reported, no such phasic negativity is observable on correct trials (Fig. 4.1A, red line).

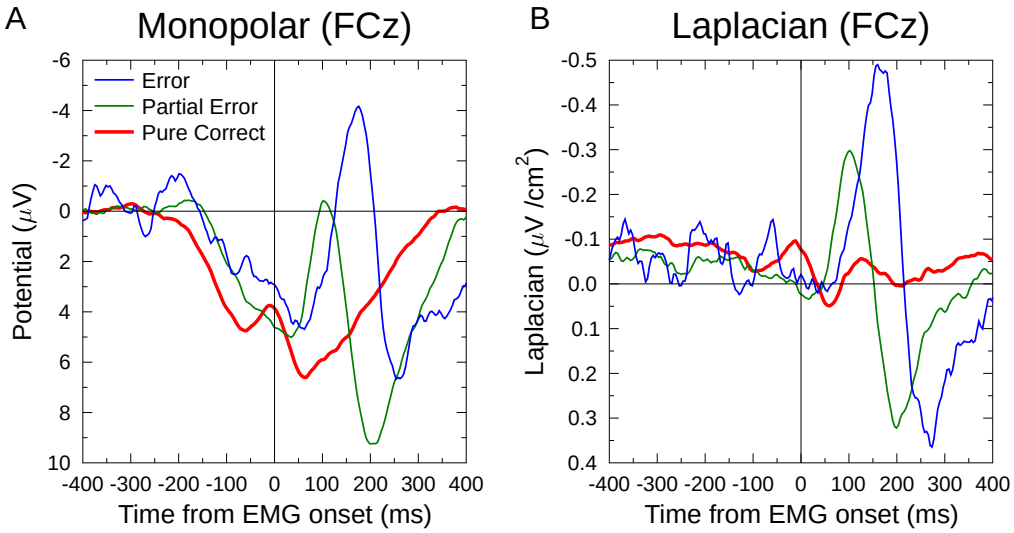

FIGURE 4.1 – **Grand averages (FCz) of the three categories of trials (Error : blue, partial error : green and pure correct : red, for the monopolar data (panel A), and for the Laplacian transformed data (panel B).** The zero of time indicates the relevant EMG onset : for correct trials, this corresponds to the EMG burst that triggered the correct mechanical response. For errors, it corresponds to the EMG burst that triggered the error. For partial errors, the relevant EMG is the small, subliminal, EMG burst occurring on the incorrect hand before the EMG burst triggering the correct response. On the monopolar data (panel A), one can clearly see the Ne for errors and partial errors, but no negativity is visible on correct trials just after EMG onset. As already reported, a large positivity is observable, instead. On the contrary, after Laplacian transform, a clear negativity, although of smaller amplitude, appears also for correct trials. The large positivity, likely generated by remote sources, has disappeared, hence allowing to reveal the small negative wave, much more focal, present on correct trials.

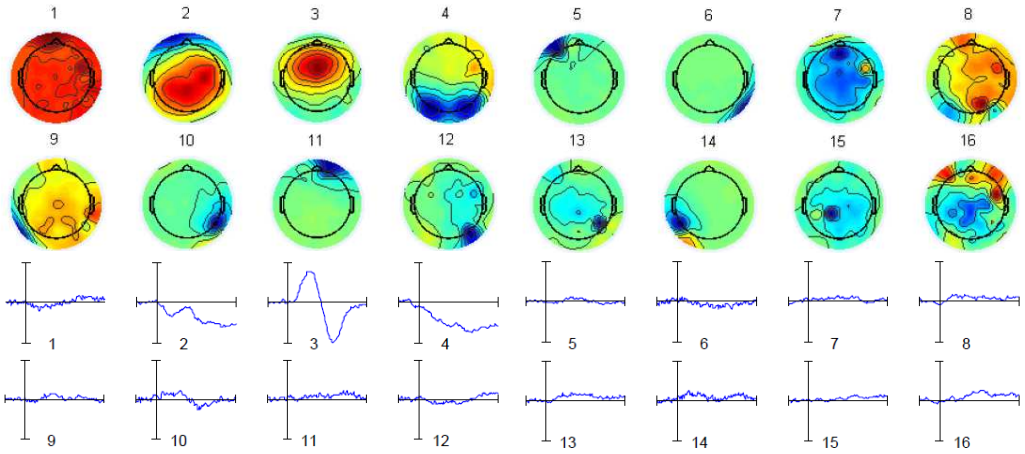

FIGURE 4.2 – **Example of decomposition and component selection for subject 01.** This figure presents the 16 first components (among 64). The first two row present the topographies of the components, and the last two rows present the corresponding averaged time courses for the same components for error trials, time locked to incorrect EMG onset. In this example, the third component clearly presents a fronto-central distribution and a clear increase in activity just after the incorrect EMG. This component was thus selected for this particular subject. The same procedure was applied to all the subjects.

Laplacian data

The Laplacian data provide a different picture : although negative waves are still clearly observable on errors and partial errors (Fig. 4.1B, lines blue and green, respectively) over FCz, a small negative activity now becomes visible on correct trials over the same electrode (red line on Fig. 4.1B), with a latency comparable to that observed for errors and partial errors. The amplitude of those negativities significantly differ across trial types ($F(2, 18) = 34.9, P < 0.001$). A latency effect of the peak also shows up ($F(2, 18) = 24.5, P < 0.001$), with a peak occurring earlier for partial error (mean latency : 109 ms) than for correct trials (mean latency : 123 ms) and errors (mean latency : 162 ms). The latency difference between partial and full errors replicates results already reported by Carbonnell et Falkenstein (2006) and extend them, by showing that the latency for correct trials lies in between partial and overt errors.

4.3.3 ICA Data

Fig. 4.2 illustrates how the component Ne_IC_{01} was selected for subject 01. This figure presents the 16 first components, with their topography (top) and their temporal dynamics on error trials

(bottom, the vertical bar indicates EMG onset). As one can easily see, the component n° 3 presents a topography and a temporal dynamic compatible with the Ne, with a large activity occurring shortly after EMG onset. This component was thus chosen as representing the Ne on errors, and will be called Ne_IC_{01}, where "01" stands for subject 01. The same procedure was applied to all the subjects, allowing to identify the $Ne\_IC_S, S \in \{1, 10\}$. Note that, during this selection stage, the time course of the components for correct and partial error trials was unknown.

Based on those criteria, we could find a component Ne_IC_S whose topography and time course could account for the Ne on errors (First step described above) for each subject. Fig. 4.3 shows the topography of all the selected Ne_IC_S for each subject S and table 4.1 gives the rank of the selected Ne_IC_S for each subject S. It is to be noted that the Ne_IC_S are always among the first components, for all the subjects (lowest rank = 9). As components are ranked according to their energy, this indicates that they account for a large part of the original signal.

Once each of Ne_IC_S had been identified, we averaged, for each subject S, the time courses of these Ne_IC_S for correct trials and partial errors. The grand average is presented in Fig. 4.4A. One can clearly see a negative activity for both partial errors and, more importantly, for correct trials, albeit of smaller amplitude [4]. Statistical analysis revealed that the amplitudes of the peaks depend on trial types ($F(2, 18) = 24.0, P < 0.001$). A latency peak effect also showed-up ($F(2, 18) = 34.5, P < 0.001$, mean latencies : 116, 111 and 162 ms for correct, partial errors and errors, respectively). For the sake of comparison, Fig. 4.4B also presents the Laplacian data plotted with the same baseline and focus. The similar statistical results, along with the comparison between panels A and B indicate a close similarity between the Laplacian data and the component isolated by ICA. We will come back on this similarity in the discussion.

4.3.4 Source Localization

Localization of the selected component

Assuming that each Ne_IC_S reflects a single neural source, one can attempt to localize the generator of the component with a single equivalent dipole. This was done for each Ne_IC_S (*i.e.* for each subject) with the "`dipfit`" module of EEGLAB. Fig. 4.5 shows the equivalent dipole located at the median position of the individual dipoles. These median positions ($x = 0.6$, $y = 4$ and $z = 36.2$, Talairach coordinates) clearly point to a source in the Rostral Cingulate Zone

4. Since the data matrix was centered on the response-related EMG, the available pre-EMG activity for partial error is shorter than for the other trials. This is why only 100 ms before EMG onset is presented

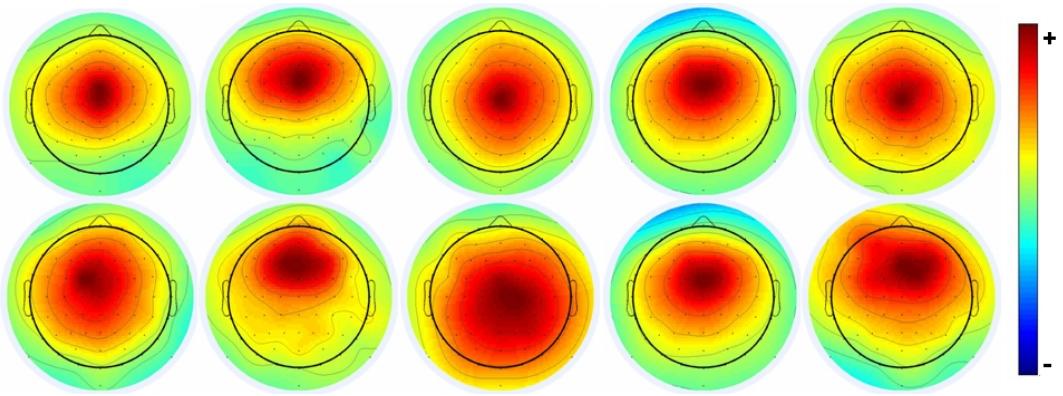

FIGURE 4.3 – **Topographies of the Ne_IC_S for each of the 10 subjects.** All of them present a fronto-central topography. Note that, although all the maps present a positive polarity, this polarity is somehow arbitrary. Indeed, the projected signal on the sensors space is the product of the topography and the time-course. Hence inverting the polarity of both the topography and the time course produces exactly the same results. For the sake of simplicity, all the topographies have thus been plotted as positive, and the time course as negative in the period of interest. Importantly, for all the Ne_IC_S, the projected activity in the sensors space was always of negative polarity at the time of the Ne.

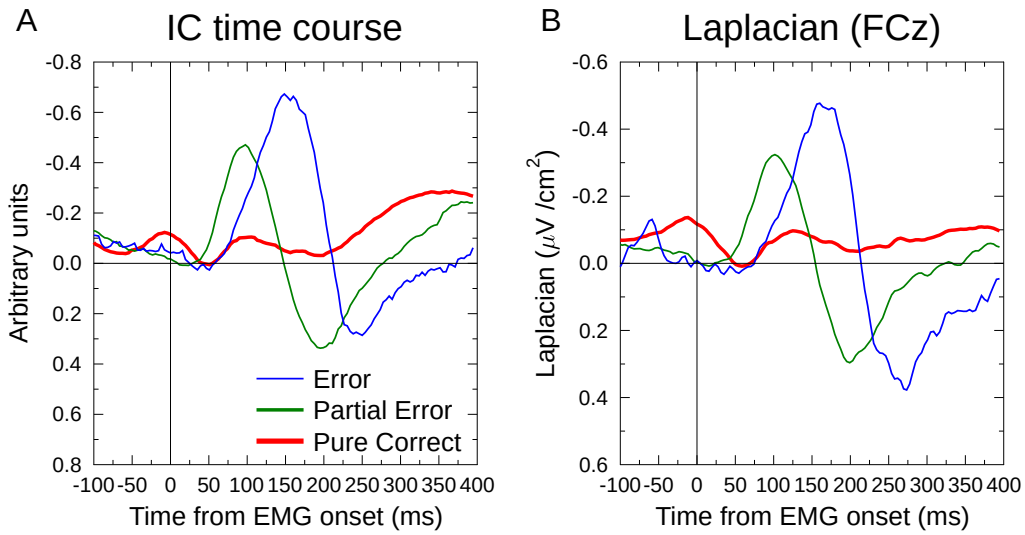

FIGURE 4.4 – **Grand average of the Ne_IC_S time course (panel A) and of the Laplacian transformed data (panel B, electrode FCz), for the three categories of trials.** The zero of time corresponds to EMG onset (see Fig. 4.1 for details). The ICA data present a clear negative activity just after EMG onset, for both the partial errors and the correct trials.

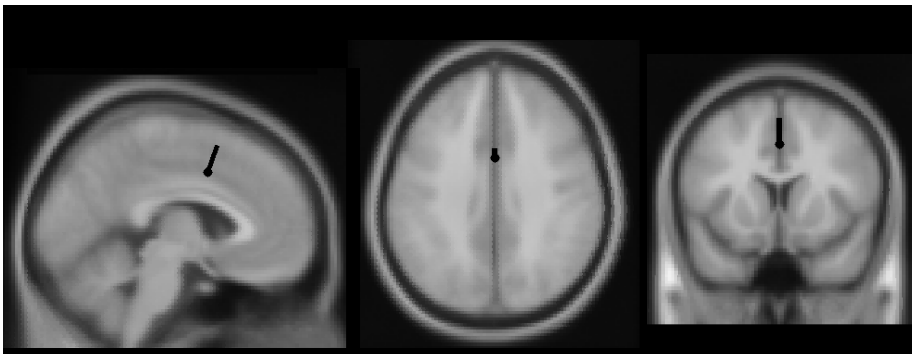

FIGURE 4.5 – **Source localization of the Ne_IC_S.** A localization of all the Ne_IC_S was performed with `dipfit` plugins of EEGLAB. The median position of all those dipoles coordinates and orientation was taken, and the equivalent median dipole is plotted in the MNI averaged brain. The equivalent dipole accounting for the Ne_IC_S is located within the RCZ.

(Ridderinkhof *et al.*, 2004a) which is very likely the generator of the Ne (Dehaene *et al.*, 1994; Van Veen et Carter, 2002; Debener *et al.*, 2005; Herrmann *et al.*, 2004).

Distributed sources Localization on the original data

The ICA data suggest that the negativities observed on errors, partial errors and correct trials are of same nature. To further establish this point, we performed a source localization of the EEG data in the time range of those negativities. The Ne on errors has already been localized, both with single dipole modeling (Dehaene *et al.*, 1994; Van Veen et Carter, 2002) and with distributed sources (Herrmann *et al.*, 2004). There is a clear agreement for a source in the RCZ, although the precise structure might still be debated.

In the present study, Source localization was performed on the grand average by using the standardized Low Resolution Electromagnetic Tomography (sLORETA) method (Pascual-Marqui, 2002), which implements a particular normalization of the minimum norm algorithm. Sources were computed at 110 ms after EMG onset. Fig. 4.6A confirms that the source of the Ne on errors is within the RCZ, in the ACC and/or in the SMA. Importantly very similar sources were found for the two other types of trials. Indeed, for both the partial errors and the correct trials, sLORETA solutions are also clearly localized in the RCZ region.

4.3.5 Lateralization of the N_C on correct trials ?

Yordanova *et al.* (2004) observed that on correct trials the Laplacian topography had a fronto central dominance with "[...] an additional tendency for a greater involvement of controlateral

Subject	Rank	R. V.	Tal. Coor.			MNI Coor.		
			x	y	z	x	y	z
01	3	4.73	0.7	5.7	36.7	46.4	66.0	57.1
02	4	2.67	0.6	-15.6	20.1	46.3	55.4	47.5
03	5	5.51	0.9	25.3	35.7	46.5	76.1	57.0
04	1	2.56	0.6	-17.4	2.5	46.3	55.0	37.9
05	2	1.99	0.6	-13.9	37.6	46.3	55.9	57.1
06	4	2.95	-15.1	5.9	36.7	38.4	66.1	57.1
07	9	4.53	0.9	23.9	18.1	46.5	75.7	47.5
08	4	5.25	0.7	2.2	1.5	46.4	65.1	37.9
09	2	3.66	0.7	5.7	36.7	46.4	66.0	57.1
10	4	5.40	0.7	-13.9	37.6	46.3	55.9	57.1
Median	-	-	0.6	4.0	36.2	46.3	65.6	57.1

TABLE 4.1 – **Summary of the equivalent dipole fitting for all the subjects.** For each subject, this table indicates the rank of the Ne_IC_S, the residual variance (R. V.), and the dipole coordinates, in both Talairach and MNI coordinates.

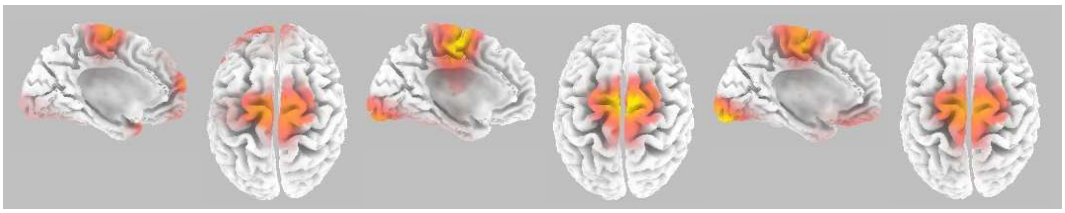

FIGURE 4.6 – **Source localization results obtained with sLORETA for errors (left), partial errors (middle) and correct (right) trials.** For the three trial types, a clear source within the RCZ was obtained.

regions [...] " (p. 594), whereas it was central on errors. This led them to conclude that the generators of the negativities in correct and error trials differ, at least partially. The finding that a single component could account for the negativities in the three categories of trials clearly speaks against different generators. Here, we explored another hypothesis, namely that the observed lateralization is due to another, lateralized, generator. If one assumes that the strength of this second generator is independent of correctness, it will largely impact the observed topography on correct trials (where the central activity is small), whereas its effect will be limited when the central activity is large (*i.e.* for errors). In order to evaluate this hypothesis we measured the activity over the FC1/FC2 electrodes (depending on response side). As a matter of fact, a clear negativity was observed over these electrodes for the three categories of trials (Fig. 4.7). Its surface (between 90 and 110 ms, around the peaks) did not vary as a function of correctness (-0.195, -0.201 and -.144 $\mu V/cm^2$ for correct, partial errors and errors, respectively, $F(2, 18) = 0.93, P = 0.41$), however. Furthermore, although the medio-central negativities present a latency shift (see above), the latency of the lateral negativities did not (103 ms, 98 ms and 104 for correct, partial errors and errors, respectively, $F(2, 18) = 0.49, P = 0.62$). This analysis confirms the presence of a negativity controlateral to the produced EMG activity for all three types of trials. Its amplitude being the same for the three categories, the lateralization is more visible for correct trials. This impression is further amplified by latency effects (see Fig. 4.8). Indeed, the FC2 activity peaking earlier than the Ne on errors, the topography at the peak of the Ne is less influenced by the lateralized activity. On the contrary, partial errors, and even more, correct trials present a greater lateralization since the time-course of the medial component is similar to the lateralized one.

4.4 Discussion

Since its discovery by Falkenstein and colleagues (Falkenstein *et al.*, 1991), the Ne has attracted a lot of interest in the cognitive control literature. Yet, its precise functional role is still unclear (Burle *et al.*, 2008a). Among open issues, the question as to whether the "Ne-like" observed on correct trials (Vidal *et al.*, 2000, 2003a; Mathalon *et al.*, 2002) is of the same nature as the Ne observed on errors and partial errors, or whether it reflects a completely different activity, is critical. We addressed this point by using the property of ICA to *blindly* identify the *elementary components* of the EEG signal. We reasoned that if the Ne on errors and on correct trials reflect the same brain activity modulated in amplitude, it should be captured in a single component by ICA. On the contrary, these negativities should be scattered into different components if they reflect completely

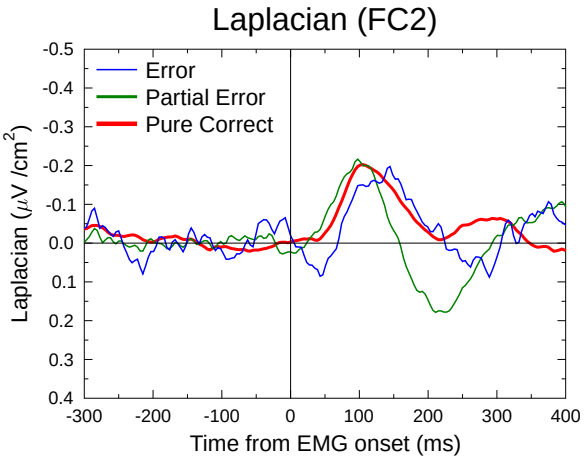

FIGURE 4.7 – **Grand average of the fronto-lateral negativity observed over FC1/FC2 (depending on response side) after Laplacian computation, for errors (blue), partial errors (green) and correct (red) trials.** This lateral activity is present for the three categories of trials, and neither its amplitude nor its latency differ across the three trial types. This activity is likely a follow-up of the negativity observed above the primary motor cortices contralateral to the response, just before EMG onset (see Burle *et al.*, 2008a, Burle *et al.*, 2004b for an overview).

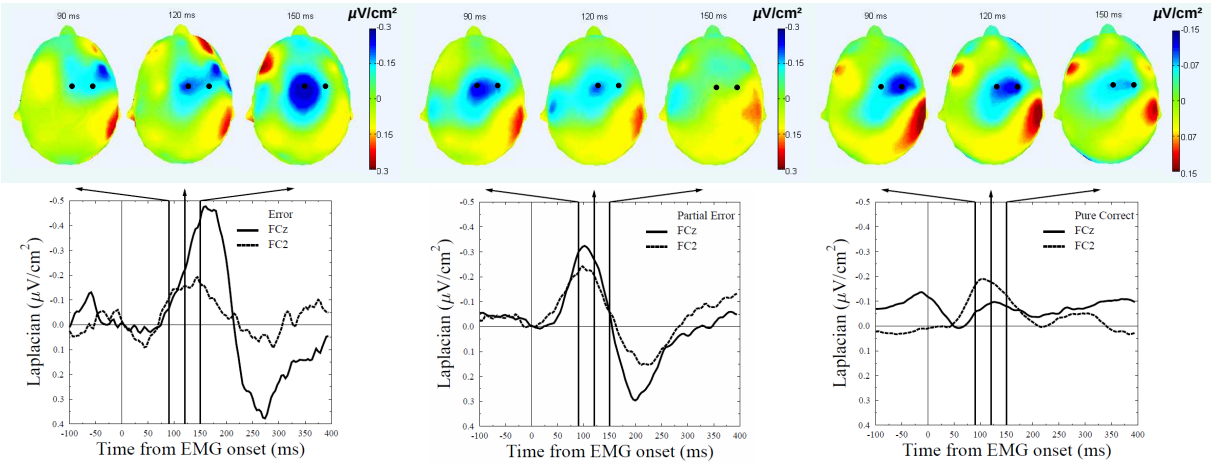

FIGURE 4.8 – **Topographies and time courses of the medial and lateral activity, for the three types of trials (error, partial errors and correct trials, from left to right, respectively.** The enhanced lateralization on correct comes from two interacting factors : first, on correct, the amplitude of the lateralized activity being closer (actually even larger) than the medial one, it largely contributes to the topography. The larger amplitudes for the medial activity on partial errors and errors, while the lateralized one does not change, reduces the impression of lateralization, although the lateralized component is of same amplitude. The second factors is timing. Indeed, the latencies of the medial activity differs across trial types, but it is not the case for the lateralized one. The peaks of the medial and lateralized activity are very similar for correct, but less so for errors, which further emphasizes the impact of the lateralized activity on correct trials.

different brain processes.

For all subjects, ICA could isolate a single component, localized within the RCZ (Fig. 4.5), accounting for the negativities in the three categories of trials (correct, partial errors and errors). In other words, ICA *blindly* attributed a single source to the negativities recorded for those three categories of trials.

Besides the ICA argument, the source localization results also point toward a unique brain activity modulated in amplitude. As already reported (Dehaene *et al.*, 1994; Van Veen et Carter, 2002; Herrmann *et al.*, 2004), the generator of the Ne on errors was located within the RCZ. The present data extend these results by locating, for the first time, the N_C within the RCZ, for both partial error and correct trials. Although a common brain source localization cannot be considered as a definitive argument for the unicity of the underlying process, this provides strong support for such a claim. Furthermore, the source of the N_C being located within the RCZ, known to be largely involved in cognitive control (Ridderinkhof *et al.*, 2004a), further supports the interpretation of the N_C in terms of cognitive control, even on correct trials, in agreement with previous data showing its sensitivity to performance (Luu *et al.*, 2000b; Allain *et al.*, 2004c). For example, Allain *et al.* (2004c), capitalizing on previous results (Ridderinkhof *et al.*, 2003), have shown that the N_C amplitude was reduced on correct trials preceding an error, hence foreshadowing the forthcoming error.

Yordanova *et al.* (2004) disputed the unicity in reporting that the N_C on correct trials was lateralized contralaterally to the produced response while the Ne on error trials was not. The present data confirm the lateralization, but also show that such a lateralization is not specific to correct trials, as it is also present on partial errors and error trials. The amplitude of the lateralized component being the same for the three type of trials (Fig. 4.7), scaling effects make this lateralization appear much stronger on correct trials. Differences in time courses further exaggerate this impression. The differential modulations, both in latency and in amplitude, of the medial and lateral components across trial types clearly indicates that they reflect different brain generators, hence confirming that the N_C is medial, as the Ne on errors, and not lateralized.

Altogether, our results clearly point to a single process whose amplitude is modulated by performance. This has important consequences for our understanding of the functional role of the RCZ, and for cognitive control in general. Indeed, instead of being specific to error (Coles *et al.*, 2001), or to conflict trials (Yeung *et al.*, 2004), it appears that the RCZ is recruited by every response activation, but that the strength of this recruitment depends on the correctness of response activation and/or the time needed to correct and erroneous activation (Burle *et al.*,

2008a). This novel view adds very strong constraints on formal models of cognitive control.

Last, our results call for a more methodological comment. The results obtained with ICA and Laplacian transform are remarkably similar. Although both techniques aim at separating the contribution of the underlying sources, they are, however, extremely different from a mathematical point of view. Indeed, ICA decomposition is mainly based on the *temporal* statistical dependence between signals recorded across sensors, while Laplacian is the second *spatial* derivative of the recorded signal. The high convergence between these two different methods cross-validates their results and strengthens the above results. It also exemplifies the danger of deriving conclusions on monopolar, mixed data, and strongly speaks for the use of deblurring methods in EEG.

Chapitre 5

Sélection de la réponse

5.1 Introduction

Dans la vie quotidienne, nous sommes très souvent amenés à prendre des décisions. Certaines nécessitent une longue réflexion tandis que d'autres doivent être prises très rapidement. Les mécanismes neuronaux impliqués dans ces deux situations sont certainement très différents. Nous nous intéressons ici à la prise de décision rapide à laquelle nous faisons appel lorsque, par exemple, nous sommes au volant d'un véhicule. En laboratoire, cette prise de décision rapide est souvent étudiée dans des tâches de Temps de Réaction (TR) à plusieurs éventualités. La pression temporelle à laquelle sont soumis les sujets, les incite à prendre leur décision le plus vite possible. Exécuter correctement la bonne réponse dans les tâches de TR de choix implique que le stimulus a été identifié, que les règles d'associations stimulus-réponse ont été utilisées pour sélectionner la réponse appropriée, et enfin que le programme moteur a été exécuté. Comment le système nerveux parvient-il à faire son choix de réponse lorsque deux réponses différentes peuvent être sélectionnées ? Ce problème intéresse les neuroscientifiques depuis longtemps. De nombreuses hypothèses ont été proposées sur le déroulement des étapes de traitement de l'information. Depuis quelques années, certaines de ces hypothèses sont implémentées dans des modèles neuromimétiques. L'étude des modèles présentée dans le chapitre 2 fait ressortir des modes de sélection de la réponse très différents. Notamment, nous pouvons distinguer ces modèles sur la base de la présence ou non d'une étape d'association Stimulus-Réponse (S-R).

Pour une classe de modèle, la décision sur la réponse est intrinsèquement liée à la décision sur le stimulus (par exemple la lettre H ou S pour la tâche d'Eriksen, voir figure 2.6 page 51). Dans